Eur. Phys. J. D **2**, 191–194 (1998)

THE EUROPEAN PHYSICAL JOURNAL D

Rapid Note

Geometrical and quantal fragmentation of optical response in Na_{18}^{2+}

A. Domps[1,a], E. Suraud[1,2], and P.-G. Reinhard[3]

[1] Laboratoire de Physique Quantique, Université Paul Sabatier, 118 Route de Narbonne, 31062 Toulouse Cedex, France
[2] Institut Universitaire de France
[3] Institut für Theoretische Physik II, Universität Erlangen–Nürnberg, Staudtstr. 7, 91058 Erlangen, Germany

Received: 6 April 1998 / Accepted: 24 April 1998

Abstract. By comparing quantal and semi-classical calculations of optical response, we work out the part of the splitting of the plasmon spectra which is exclusively due to geometrical effects. We apply the analysis to the test case Na_{18}^{2+} which exhibits an interesting geometry with strong prolate quadrupole deformation and a pronounced asymmetry in addition. We find a new type of resonance splitting which is due to geometrical effects but goes beyond the simple and well known deformation splitting.

PACS. 36.40.Vz Optical properties of clusters – 36.40.Gk Plasma and collective effects in clusters – 36.40.Mr Spectroscopy and geometrical structure of clusters

1 Introduction

The optical response has since long been employed as a valuable tool to investigate the structural properties of free metal clusters [1–4]. It delivers also decisive signatures for the deformation of clusters on surfaces [5]. And it may be extremely worthwhile for tracing the shape evolution during cluster fission [6]. The average plasmon position as such is dictated by the material and a bit by the system size. The indicators for the underlying structure are taken from the detailed pattern of the resonance spectrum. Two basic mechanisms are known to determine the spreading of the resonance. There is first a collective splitting of the resonance into different x-, y-, and z-modes being uniquely related to the overall quadrupole deformation of the ionic background in that the eigenfrequencies of the dipole response roughly scale with the inverse length of the axes [3]. This has been exploited extensively to measure the deformation systematics of clusters [7]. There is, on the other hand, often fine structure in the spectra from a much different origin, namely a Landau fragmentation due to coupling of the resonance to energetically close $1ph$ states. This is a quantum effect related to the quantal level density of the system. The Landau fragmentation is often washed out to a mere broadening of the resonance and the interplay between collective splitting and Landau damping determines the actual plasmon width including its temperature dependence [8]. The question remains whether this is all or whether there are other mechanisms for a resonance splitting conceivable. A positive answer is hinted by the example of asymmetric fission [6]. The different final fragments carry each their own plasmon frequency which adds up in the spectrum to multiply split resonances. This feature presumably continues to more merged configurations where the clusters are still in contact and the splitting thus has to be interpreted as a new sort of splitting wich is due to the peculiar fission shapes. It seems in such situations that the electron cloud does not vibrate as a whole all over the cluster but that the collective oscillation rather takes place on localized "subensembles".

It is the aim of this paper to search for such geometrical splitting in ground state clusters and to investigate such an effect in detail. As test case, we consider the prolate ground state of Na_{18}^{2+} which seems to indicate already a trimer waiting for asymmetric fission [9]. The theoretical tool for the study is the comparison of a fully quantal computation of the spectra within the time-dependent local-density approximation (TDLDA) with its semiclassical counterpart at the level of the time-dependent Thomas-Fermi approximation (TDTF) [10]. The TDLDA gives the full spectrum containing all geometrical splitting effects together with Landau fragmentation. We treat it here in a fully fledged time dependent basis with the meanwhile well tested methods of [11]. The TDTF, on the other hand, can only cover the geometrical effects and is free from any $1ph$ fragmentation. This allows to discriminate the geometrical effects. Practically, TDTF is handled with much

[a] e-mail: adomps@irsamc2.ups-tlse.fr

similar numerical techniques [12] which puts the comparison on safe grounds.

The paper is organized as follows. We first briefly outline the TDLDA and TDTF formalisms (Sect. 2). We then discuss as a typical test case the Na_{18}^{2+} cluster in its prefission ground state (Sect. 3) and we analyse geometrical effects from the velocity spectra (Sect. 4). In Section 5 we see how such an analysis provides a tool for understanding the optical response. We finally give conclusions in Section 6.

2 Model and observables

We take TDLDA as starting point for the description of electron dynamics which represents the simplest version of time-dependent density functional theory [13] and which has been used with success in its linearized version [1,4] as well as in its fully nonlinear form [11,14,15]. In fact, the high precision of the codes for full TDLDA allows also computations in the linear regime of small amplitudes [16] and the coding of full TDLDA is much simpler than of its linearized version such that it is easier to change approximations and ionic structure. The extraction of spectral properties from TDLDA is discussed extensively in [11].

Semiclassical approximations can be derived from TDLDA at various levels. The conceptually simplest one is the Vlasov-LDA, which has also been used with some success in cluster physics [17,18]. The Vlasov-LDA nevertheless raises formal and technical difficulties [19]. It turns out, however, that the dynamical response in metal clusters is to a large extent dominated by the dipole channel which can be described remarkably well in a TDTF frame (equivalent to a hydrodynamical picture) [12]. The TDTF provides a good approximation to the gross features (collective flow) of TDLDA. It furthermore represents the simplest version of time-dependent density-functional theory and constitutes as such an interesting topic of investigation. We shall hence rely on this approximation as an efficient and simple semi-classical approximation. By construction, TDTF misses $1ph$ effects (quantal effects are reduced here to the Pauli principle used to evaluate the kinetic energy at the Thomas-Fermi level). It is thus an ideal level of approximation which includes the proper geometrical effects but no detailed fragmentation pattern.

As we aim at discussing the effects of the cluster's geometry, we shall include explicit ionic positions by means of pseudopotentials. We use the local pseudopotentials of [16] which have been constructed ad hoc to deliver a fair reproduction of experimental optical response. In the direct time dependent formalisms used here, the optical response is accessed to *via* the dipole moment of the electronic distribution, which is recorded in time as $D(t)$. Switching to the frequency domain yields $D(\omega)$ which provides the strength function $S(\omega) \propto \mathcal{R}(D(\omega))$, directly linked to the photoabsorption cross section, and to the power spectrum $\mathcal{P}(\omega) = |D(\omega)|^2$, for details see [11]. The TDTF equation is solved by means of the Madelung transform [20], which maps TDTF into an effective time dependent Schrödinger equation, which in turn can be numerically solved with the same safe and robust technics as used in solving TDLDA [12].

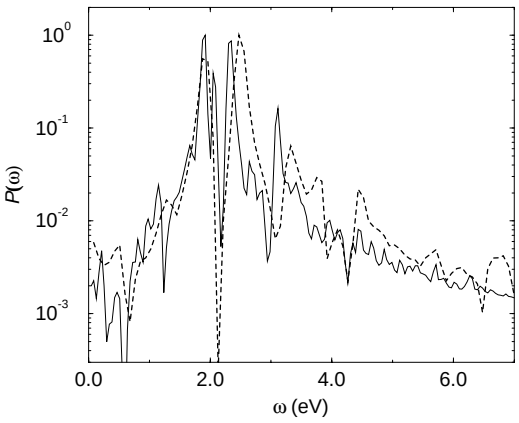

Fig. 1. Dipole power spectra in Na_{18}^{2+} for plasmon oscillation along the elongation axis, as computed within TDLDA (full line) and TDTF (dashed line).

3 A typical example

As a typical example of a cluster producing fuzzy optical response we take the ground state configuration of the Na_{18}^{2+} cluster. This cluster is interesting as it leads to competing fission channels $Na_{18}^{2+} \to Na_3^+ + Na_{15}^+$ and $Na_{18}^{2+} \to Na_9^+ + Na_9^+$ which correspond to basically different optical responses [6]. A better understanding of the (complicated) optical spectra could thus allow to identify the scission point and even give access to dynamical effects due to friction [21]. Here we restrict the considerations to the ground state which has already an interesting shape hinting a preformed trimer awaiting its release in asymmetric fission. The ionic configuration has been taken over from the cylindrically averaged pseudopotential scheme (CAPS) [9] and we restrict our analysis to the longest axis of the cluster, in order to avoid mixing with the "trivial" deformation splitting through different modes along different principle axes.

The dipole spectra from TDLDA and TDTF are shown in Figure 1. The TDLDA spectrum is highly fragmented but one can identify two groups of peaks, one centered around $\omega_1 = 2.3\,\mathrm{eV}$ and another one around $\omega_2 = 1.9\,\mathrm{eV}$. The low frequency of both groups reflects the elongated (prolate) shape of the ionic/electronic configurations. The TDTF spectrum, on the other hand, displays two well separated peaks which agree nicely with the two groups of TDLDA peaks. The detailed substructure of each peak is lost in TDTF due to the deliberate suppression of quantal effects in this scheme. Furthermore, the remaining splitting of the TDTF spectrum cannot be a simple "principal axis" effect as we have confined the consideration to the z-mode alone. Transverse modes are, as can be checked, not

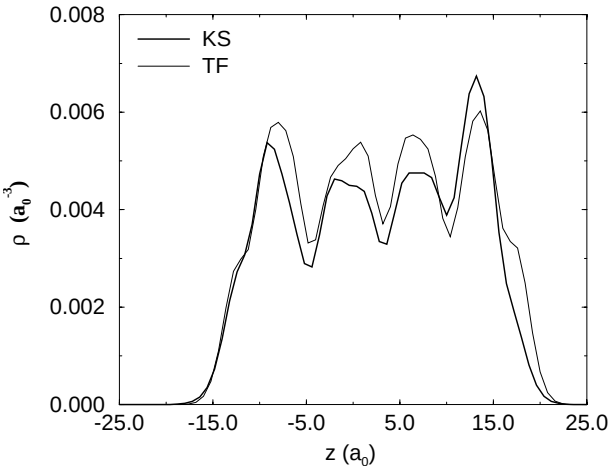

Fig. 2. Ground state electron density in Na_{18}^{2+}, as computed within Kohn-Sham (thick line) and Thomas-Fermi (thin line).

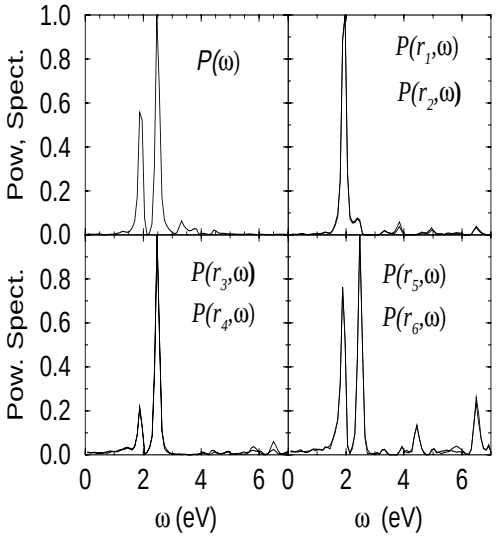

Fig. 3. Dipole power spectrum $\mathcal{P}(\omega)$ (upper left) and velocity power spectra $\mathcal{P}_v(\mathbf{r}_i, \omega)$ at various test-points $\mathbf{r}_i$ in Na_{18}^{2+}.

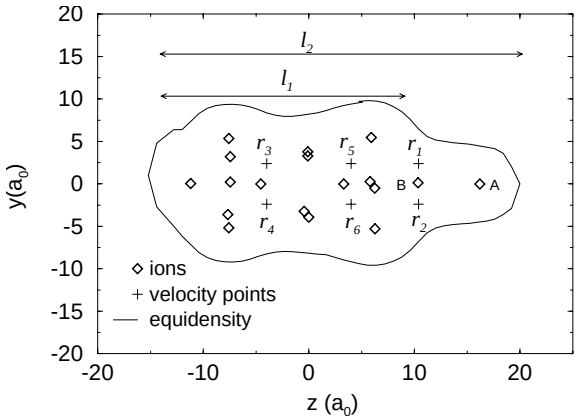

Fig. 4. Ionic structure of Na_{18}^{2+} (diamonds) and test-points $\mathbf{r}_i$ (+) chosen to compute the local velocity field. An electron isodensity line is also shown, with its two typical lengths l_1 and l_2.

excited. Still, we obtain the *a priori* surprising result that the semi-classical TDTF spectrum splits into two contributions and we expect that this splitting is of some geometrical origin yet to be worked out.

4 Velocity analysis of the optical response

In order to understand the peak splitting in TDTF we analyse the local distribution of the motion. First, we check the initial electronic cloud by plotting its density along z as it emerges from quantal LDA and from semi-classical Thomas-Fermi approximation. These densities are shown in Figure 2. Both densities display large oscillations associated to the ionic positions and they are much similar to each other which demonstrates that the present version of TDTF manages to reproduce the smoothness of a quantal distribution correctly. A remark is in order here: the Thomas-Fermi approach at lowest level delivers a density which vanishes abruptly at the classical turning points. We use here an effective "extended" Thomas-Fermi scheme which adjusts the Madelung term in the equivalent Schrödinger equation to cure this defect [12].

Now that we are confident with the TF representation of the quantal density we can try to analyse in more detail the origin of the peak splitting. For this purpose we consider the local velocity flow $\mathbf{v}(\mathbf{r}, t)$. From $\mathbf{v}(\mathbf{r}, t)$ we obtain by Fourier transform the corresponding velocity spectra $\mathcal{P}_v(\mathbf{r}, \omega) = |\tilde{\mathbf{v}}(\mathbf{r}, \omega)|^2$ which we compare to the dipole power spectrum $\mathcal{P}(\omega)$. The velocity spectra provide a local picture of the flow and allow to evaluate the degree of collectivity of the electronic motion. The velocity spectra of a few selected points $\mathbf{r}_i$ are plotted in Figure 3, together with $\mathcal{P}(\omega)$ for comparison. These points $\mathbf{r}_i$ have been selected in various space regions in order to see to what extent they do all oscillate at the same pace. They are shown in Figure 4 against the ionic configuration. While $\mathbf{r}_1$ and $\mathbf{r}_2$ are located at the top of the cluster ($z > 8a_0$), $\mathbf{r}_3$ and $\mathbf{r}_4$ stand deep in the core of the ionic structure ($z \simeq -5a_0$), and $\mathbf{r}_5$ and $\mathbf{r}_6$ have been chosen in an intermediate position. The results from this local analysis of collectivity are quite telling: one observes in Figure 3 that the two major peaks in $\mathcal{P}(\omega)$ are very unevenly shared among the selected points. The vibration at frequency ω_1 is much suppressed in $\mathcal{P}_v(\mathbf{r}_1, \omega)$ and $\mathcal{P}_v(\mathbf{r}_2, \omega)$, all the spectral weight being concentrated around ω_2. At the opposite, ω_1 shows up very intensely in $\mathcal{P}_v(\mathbf{r}_3, \omega)$ and $\mathcal{P}_v(\mathbf{r}_4, \omega)$, accompanied by a smaller, yet non negligible contribution at ω_2. Finally, points $\mathbf{r}_5$ and $\mathbf{r}_6$, located at intermediate positions, exhaust well balanced velocity spectra, supporting the whole picture. Thus, the vibration at ω_2 can be interpreted as a plasmon along the whole cluster, whereas the ω_1 contribution in $\mathcal{P}(\omega)$ stems from a plasmon restricted to the core part of the cluster. These results were confirmed by systematically computing $\mathcal{P}_v(\mathbf{r}, \omega)$ at more than 30 points $\mathbf{r}_i$ inside the electron cloud. We therefore associate ω_1 and ω_2 to the two typical lengths l_1 and l_2 characterizing the cluster shape along z-axis, as shown in Figure 4. This view is counterchecked by the relative

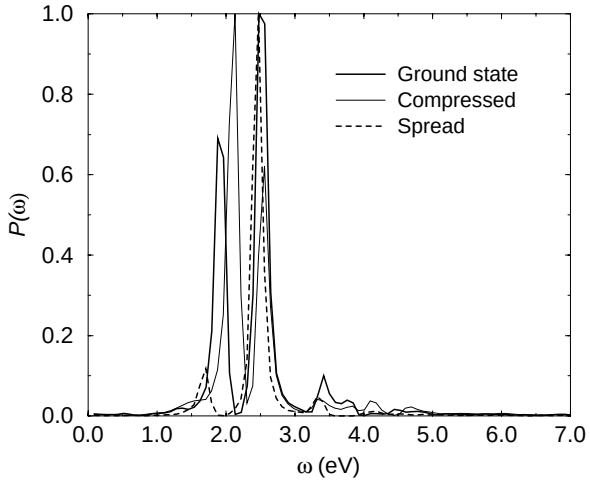

Fig. 5. Dipole power spectra in Na_{18}^{2+} for 3 different ion configurations: ground state (thick line), compressed (thin line) and spread (thick dashed line).

value of these two frequencies: the fastest oscillation is associated to the shortest length. Remind that in a three-dimensional ellipsoidal cluster, plasmon oscillations along orthonormal principal axis decouple from each other. This gives rise to a geometric splitting in $\mathcal{P}(\omega)$, associated to the existence of 3 different lengths for the principal axis. What we are seeing here is a the decoupling of 2 vibrations along *one and the same axis*, but also of a *geometric* origin.

5 Sensitivity to ionic structure

In order to confirm the relevance of the above analysis we shall now modify the actual ionic positions. This should allow to better understand the shape dependence of the response, which might be relevant, for example for tracing fission pathes. Again, TDTF is particularly suited for that purpose because is washes out quantal effect, thus providing filtering on the geometrical effects of optical response. We consider two arbitrarily deformed configurations built from the Na_{18}^{2+} ground state ionic configuration by moving ions A and B (Fig. 4) along the z direction, further inside or outside the cluster. This means that the z-axis l_2 of the cluster becomes shortened or elongated, l_1 remaining unchanged. This in turn should shift the lowest frequency ω_1 up or down. The results obtained from TDTF computation are plotted in Figure 5 and show the predicted trends: while the high energy peak at ω_1 remains essentially unaffected, we see a significant redshift of the low energy energy vibration with increasing l_2. From the original value $\omega_2 = 1.9\,\mathrm{eV}$, it decreases to 1.7 eV in the spread ionic configuration and reaches 2.1 eV if the cluster is compressed. Another striking feature from Figure 5 is the gradual extinction of the ω_2 peak with increasing l_1. This is explained as follows: moving ions A and B separates more or less a small appendix of the cluster from its core part. In the limit of very large separation, the collective plasma oscillations along the whole cluster become meaningless and only the ω_1 peak survives.

6 Conclusions

We have investigated the influence of cluster geometry on the splitting of the plasmon response. Geometrical effects have been disentangled from particle-hole fragmentation by comparing quantal TDLDA to semi-classical TDTF calculations. The simplest geometrical splitting due to overall quadrupole deformation has been suppressed by considering the modes only along one axis (here the axial symmetry axis). Nonetheless, we see a collective splitting for the ground state of Na_{18}^{2+} which is induced by geometrical effects. The cluster shows almost a trimer on its top and correspondingly there emerge two length scales, the extension all over the cluster including the top *versus* the extension of the "core". And these two length scales produce each their own plasmon response. This effect has been checked further by dilating or compressing the ionic configuration. The result suggests that similar (or even more involved) geometrical splittings may appear in other systems with non-trivial shapes, as *e.g.* for fissioning clusters or complexes of clusters on surfaces.

We thank Inst. Univ. de France and program PROCOPE (#95073) for financial support.

References

1. W. Ekardt, Phys. Phys. Rev. Lett. **21**, 1925 (1984).
2. D.E. Beck, Sol. St. Comm. **49**, 381 (1984).
3. W. de Heer, Rev. Mod. Phys. **65**, 611 (1993).
4. M. Brack, Rev. Mod. Phys. **65**, 677 (1993).
5. C. Kohl *et al.*, to appear in Surf. Science (1998).
6. P.-G. Reinhard *et al.*, Z. Phys. D **41**, 151 (1997).
7. P. Meibom *et al.*, Z. Phys. D **40**, 258 (1997).
8. B. Montag *et al.*, Phys. Rev. B **51**, 14686 (1995).
9. B. Montag, P.-G. Reinhard, Phys. Rev. B **52**, 16365 (1995).
10. S. Lundqvist, N.H. March (Ed.), *Theory of the inhomogeneous electron gas* (Plenum Press, 1983).
11. F. Calvayrac *et al.*, Ann. Phys. **254**, (N.Y.) 125 (1997).
12. A. Domps *et al.*, to appear in Phys. Rev. Lett. (1998).
13. B. Runge *et al.*, Phys. Rev. Lett. **52**, 997 (1984).
14. F. Calvayrac *et al.*, Phys. Rev. B **52**, R17056 (1995).
15. K. Yabana *et al.*, Phys. Rev. B **54**, 4484 (1996).
16. F. Calvayrac *et al.*, J. Phys. B (in press).
17. M. Gross, C. Guet, Z. Phys. D **33**, 289 (1995).
18. L. Féret *et al.*, J. Phys. B **29**, 4477 (1996).
19. A. Domps *et al.*, Ann. Phys. (Leipzig) **6**, 468 (1997).
20. E. Madelung, Z. Phys. **40**, 322 (1927).
21. P. Fröbrich, Z. Phys. D **40**, 198 (1997).
22. G.F. Bertsch, R. Broglia, *Oscillations in finite quantum systems* (Cambridge Univ. Press, 1994).
23. J. Babst, P.-G. Reinhard, Z. Phys. D **42**, 209 (1997).